Supplementary information:

Spatial Reorganization of Analytes in Charged Aqueous Microdroplets

Pallab Basuri, Amrita Chakraborty, Tripti Ahuja, Biswajit Mondal, Jenifer Shantha Kumar, and Thalappil Pradeep*

1 DST Unit of Nanoscience (DST UNS) and Thematic Unit of Excellence (TUE), Department of Chemistry, Indian Institute of Technology Madras, Chennai 600 036, India

Correspondence to: pradeep@iitm.ac.in

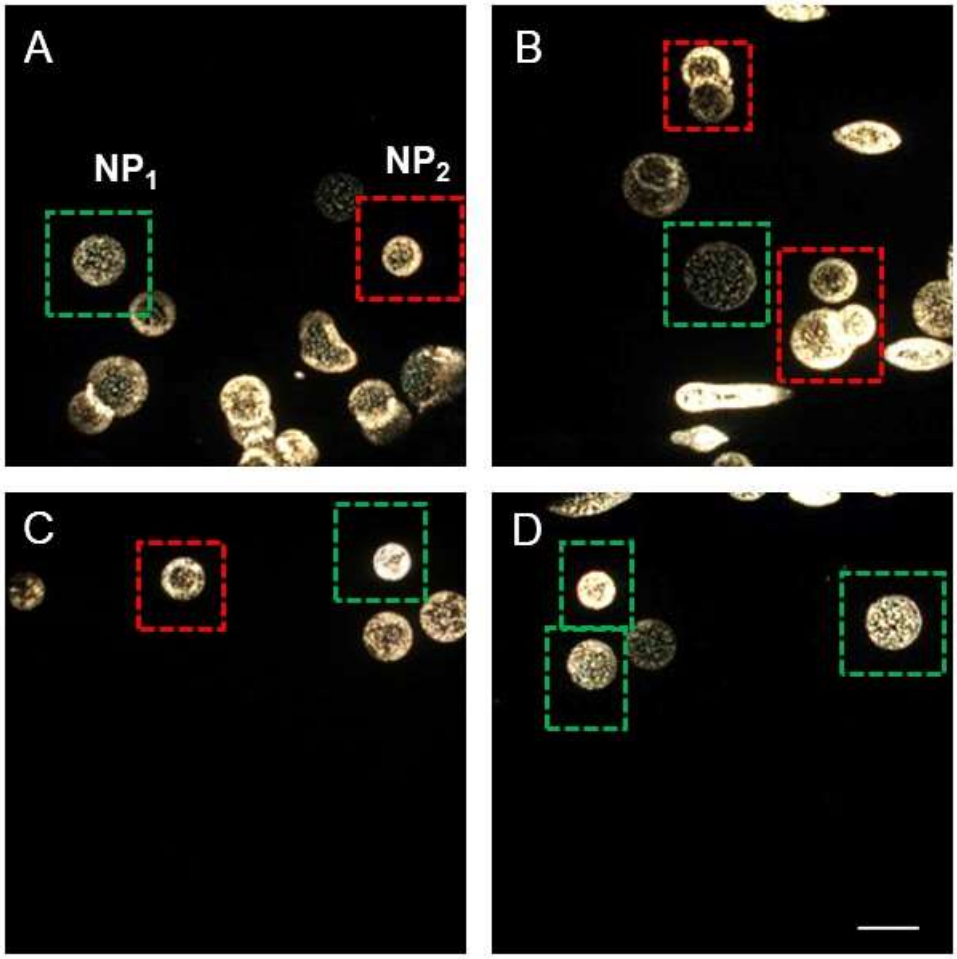

Fig. S1 DFM images of microdroplets containing AgNPs in water, from different regions of the slide. Both NP1 and NP2 can be observed in all four images and are indicated by green (NP1) and red (NP2) squares. A-D) Images taken from different locations of the sample. The scale bar shown here is 100 μm.

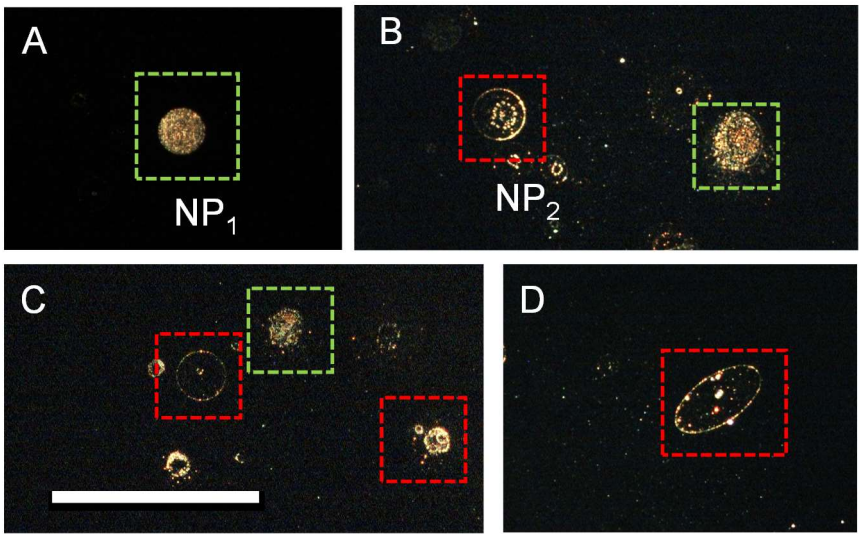

Fig. S2 DFM images of microdroplets containing AuNPs in water. Both Type NP1 and NP2 can be observed in all four images and are indicated by green (NP1) and red (NP2) squares. A-D) Images taken from different locations of the sample. The scale bar shown here is 250 µm.

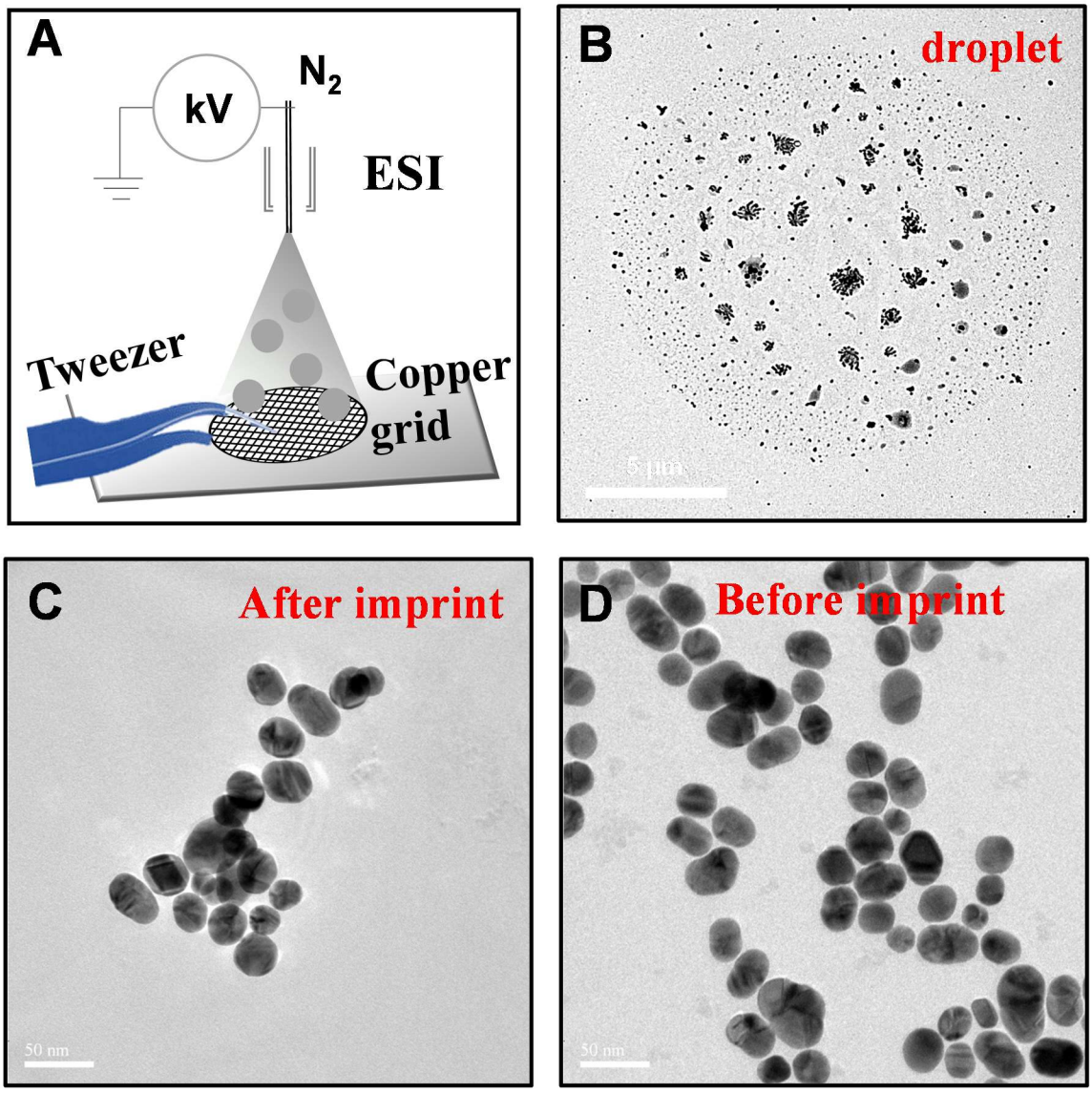

Fig. S3 Transmission electron microscopy of imprinted droplets containing aqueous colloidal AuNPs. (A) Schematic view of the experimental setting of droplet imprinting in a TEM grid. (B) TEM image of a droplet (NP2). Clustering of AuNPs was also observed at the interior of the droplet. The scale bar shown here is 5 µm. (C-D) TEM images of AuNPs before and after spray at higher magnifications. The scale bar shown here is 50 nm. Approximately 10 µL of AuNPs dispersion were drop casted and dried on a TEM copper grid before the imprint experiments.

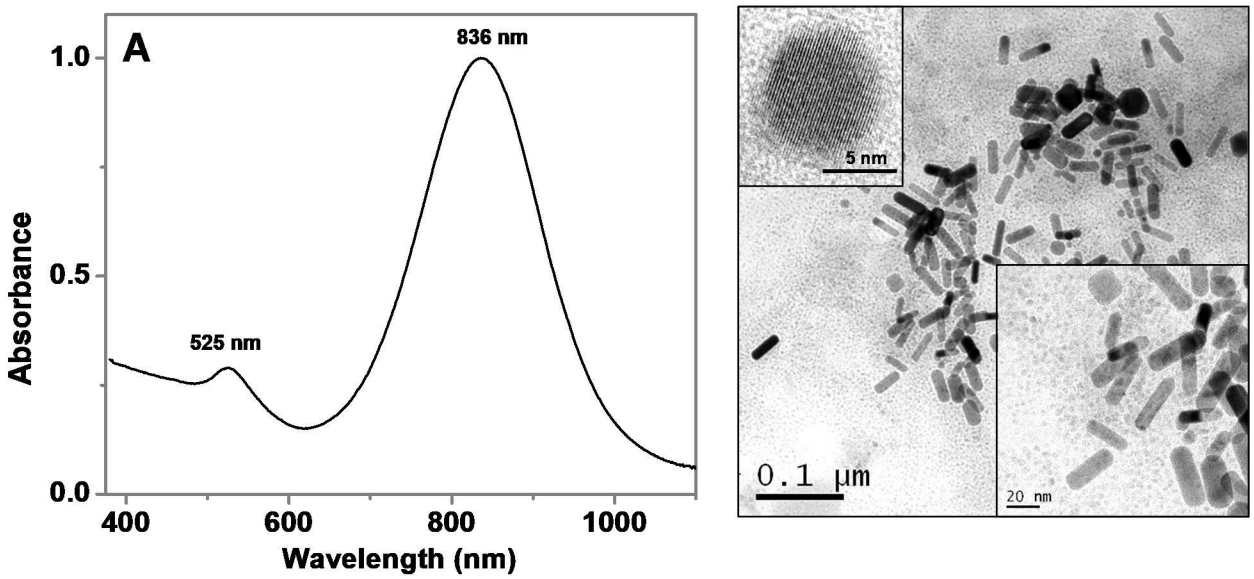

Fig. S4 Characterization of as-synthesized gold nanorods. (A) UV Vis spectroscopy of GNRs showing two characteristic peaks at 525 and 836 nm. (B) TEM characterization of gold nanorods. The TEM image shows the impurity of AuNPs of different sizes and shapes.

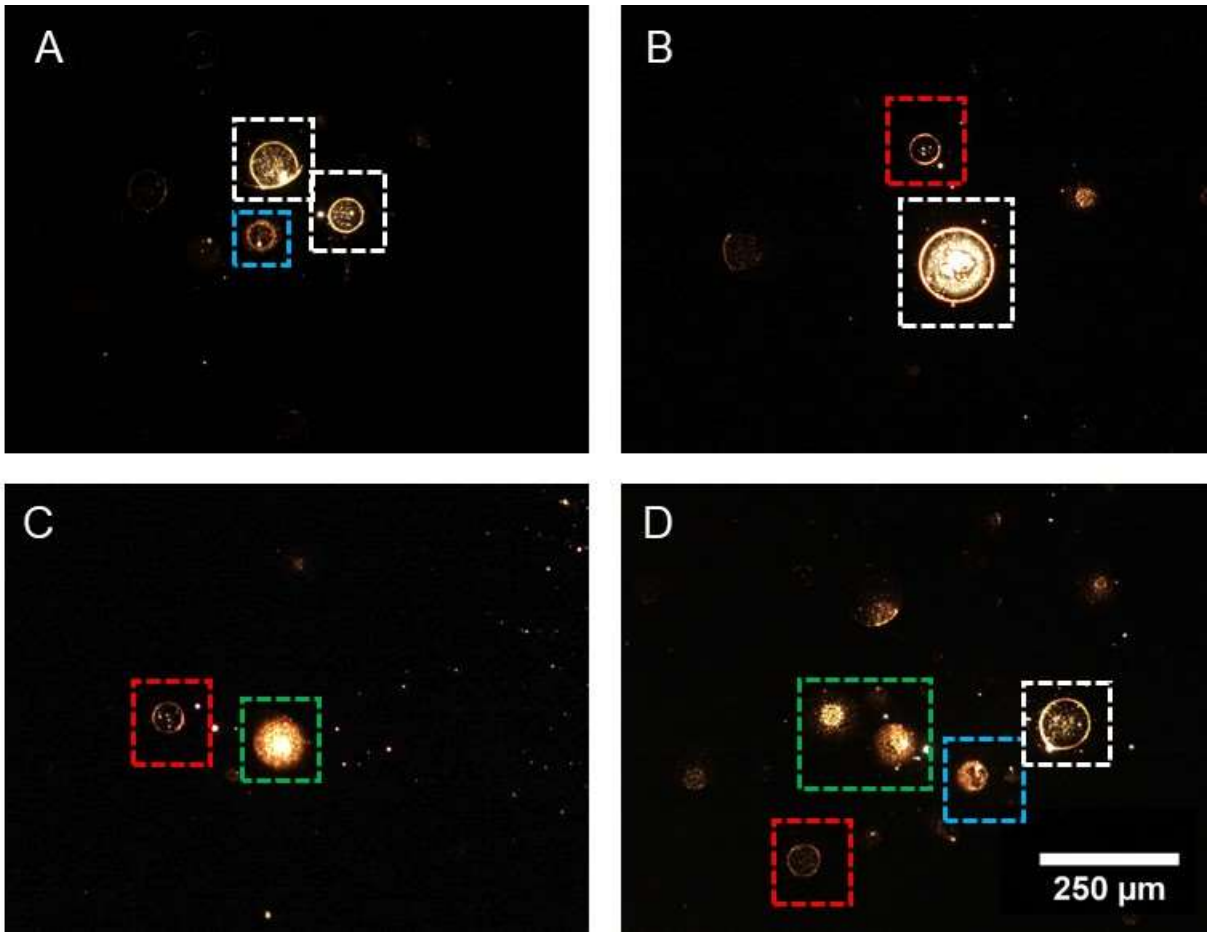

Fig. S5 DFM images of the imprinted droplets containing as-synthesized GNR. These droplets were produced with electrospray parameters of 1.5 kV applied potential and 20 psi nebulization gas pressure. The droplets were imprinted at a 2.5 cm distance from the tip. A-D) Images from different location of sample. Different types of droplets such as Mix1-Mix4 were marked with green, cyan, white, and red squares.

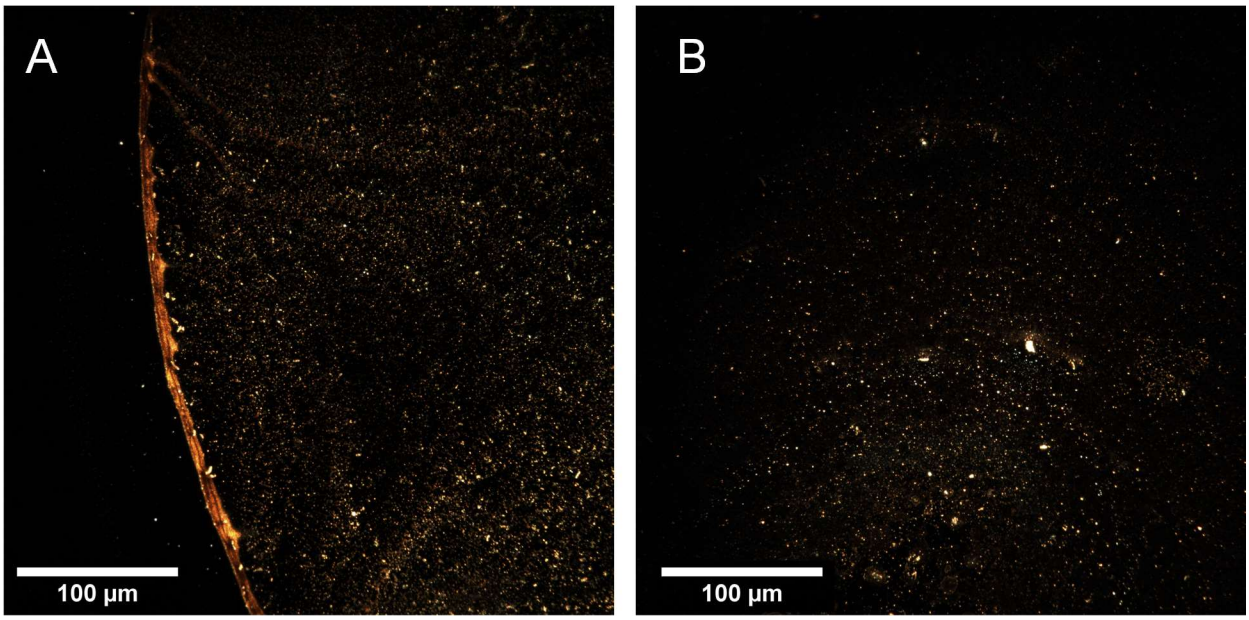

Fig. S6 DFM of the drop casted sample of 10 µL of bulk solution on a glass surface. A coffee ring was observed with higher concentration of particles at the periphery of the dried drop (A). However, no unique particle distribution and vacuoles were observed at the interior (B).

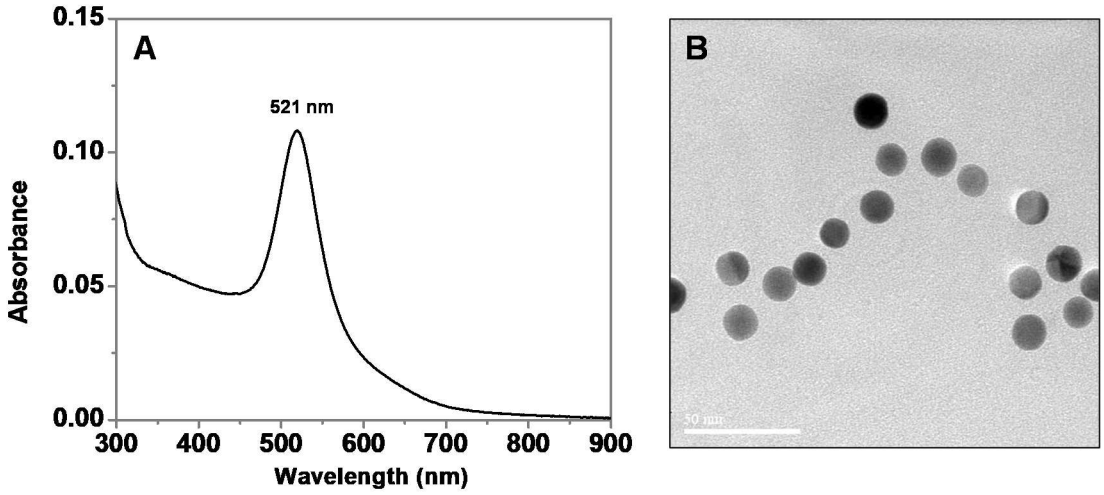

Fig. S7 Characterization of as-synthesized CTAC-protected AuNPs. (A) UV Vis spectroscopy of AuNPs showing a characteristic peak at 521 nm. (B) TEM characterization of AuNPs.

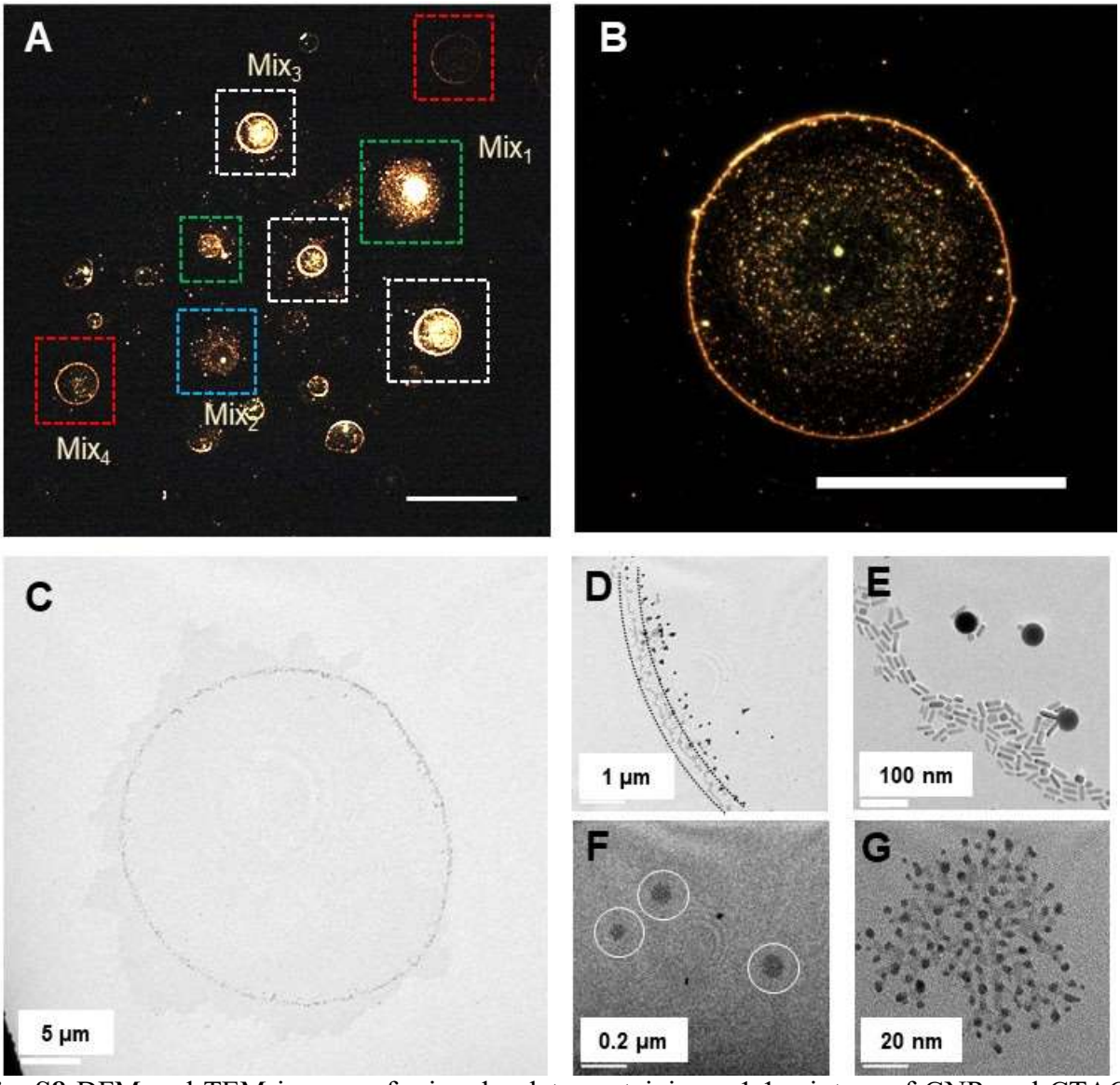

Fig. S8 DFM and TEM images of microdroplets containing a 1:1 mixture of GNR and CTAC-protected AuNPs in water. (A) Different types (Mix1-Mix4) of droplets. Distributions of similar types are marked with the same colored squares. The scale bar shown here is 250 µm. (B) Zoomed-in image of a droplet of Mix3. The scale bar shown here is 100 µm. (C) TEM image of a droplet showing enrichment of GNRs and MBA protected-AuNPs at the periphery (D and E) along with clusters of nanoparticles at the interior (F and G).

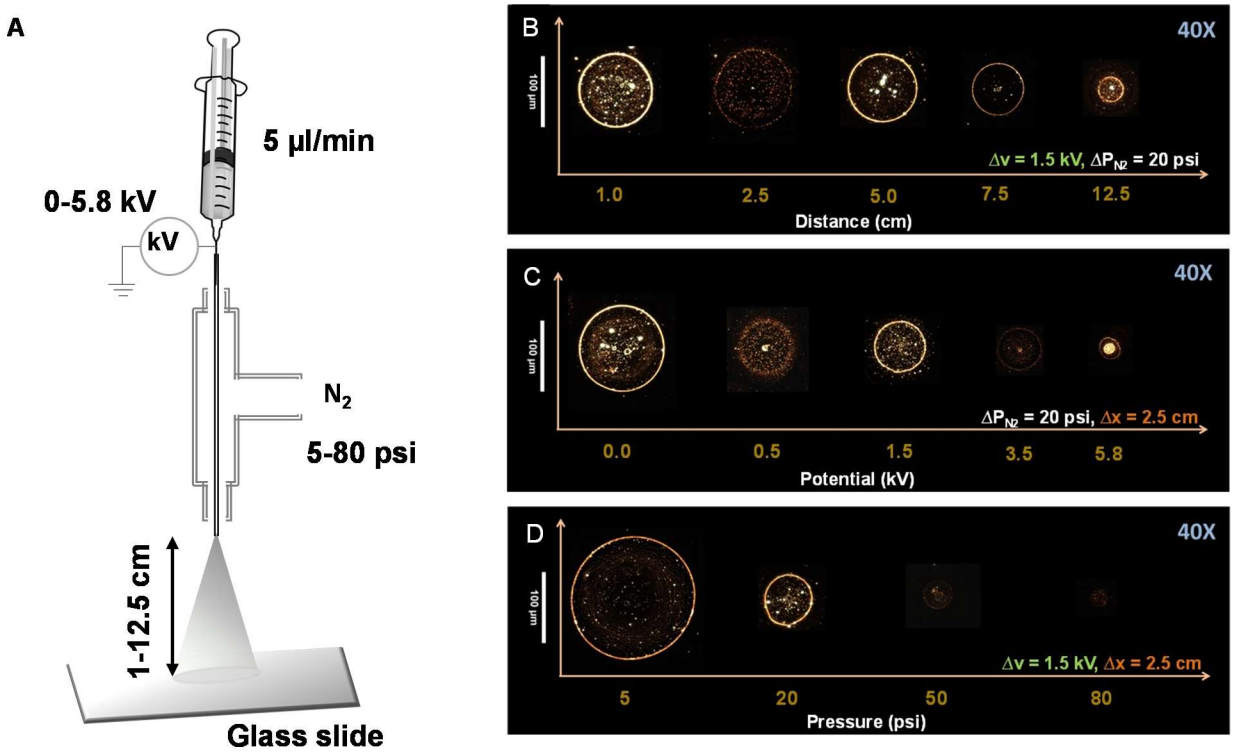

Fig. S9 Effect of ESI parameters on the droplet size. (A) Schematic representation of the experimental settings. Three parameters such as tip-to-surface distance, spray potential, and nebulization gas pressure were varied. One parameter was varied at a time, keeping all others fixed. DFM images of droplets with varying tip-to-surface distance (B), potential (C), and nebulization gas pressure (D). We showed one representative droplet per parameter investigated. The scale bar is 100 µm.

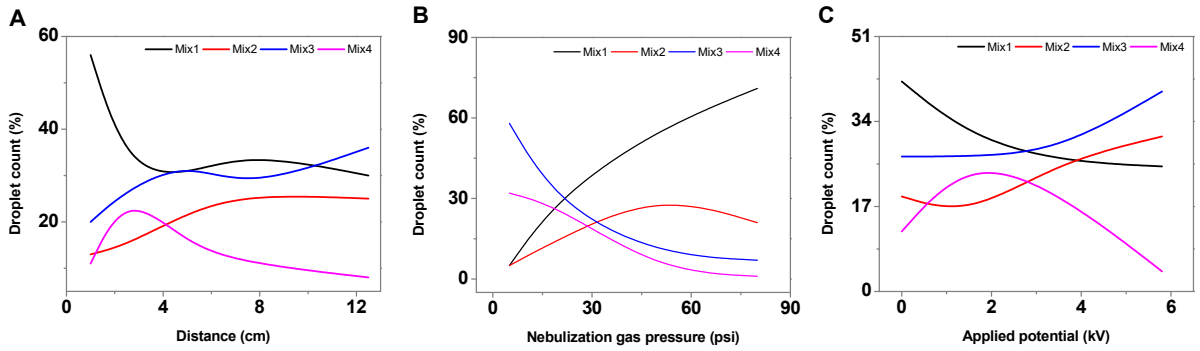

Fig. S10 Statistical analysis of droplet type distribution at various ESI parameters such as A) distance, B) nebulization gas pressure, and C) applied potential. Particle redistribution occurs with increasing distance and applied potential and with decreasing gas pressure. This hints at the fact that applied potential and tip-to-deposition distance are the two major factors behind particle relocalization within the droplet.

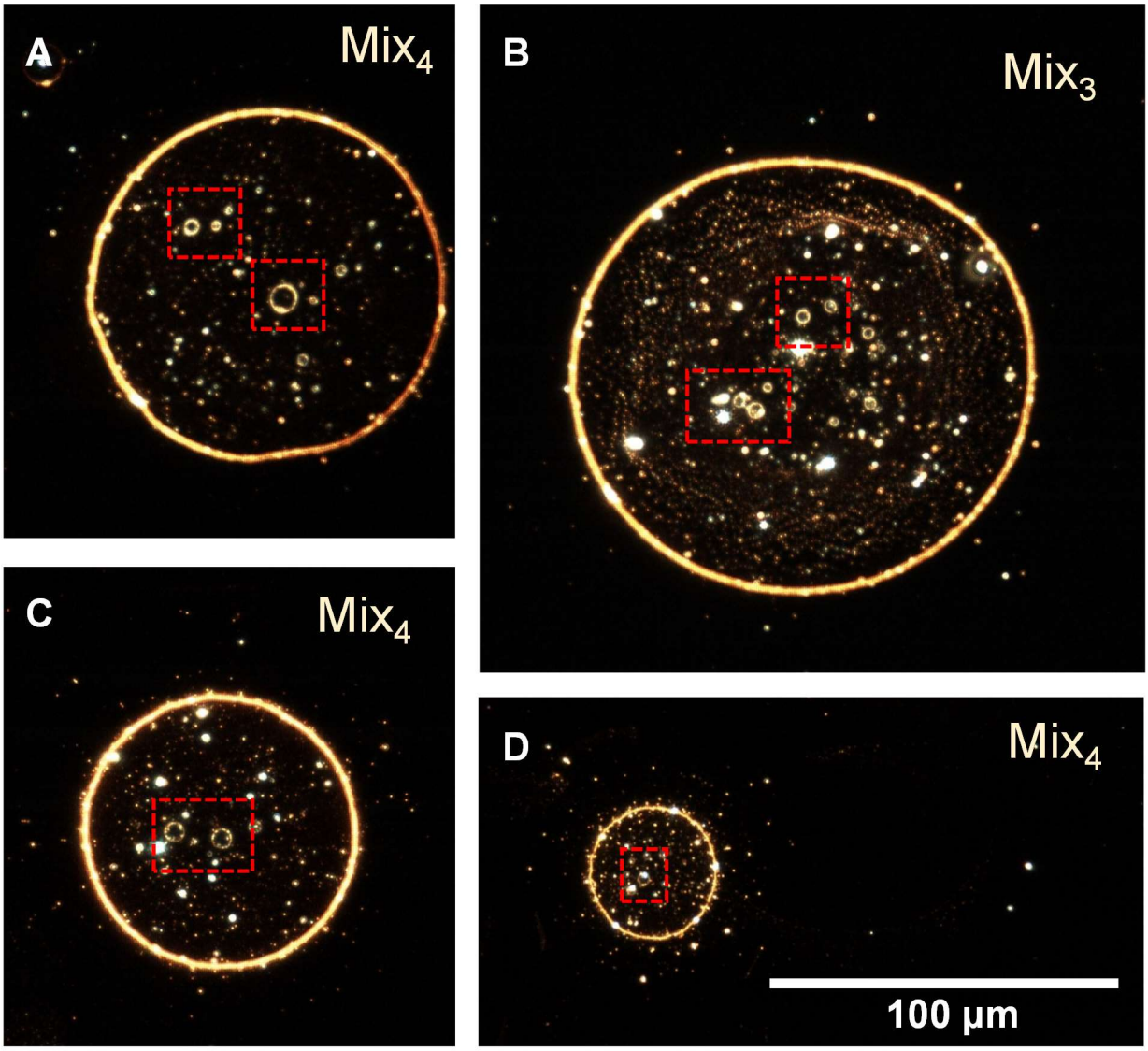

Fig. S11 Vacuolization in aqueous microdroplets. Microvacuoles in the DFM images of the droplets of as-synthesized GNR are indicated with red squares. Single or multiple vacuoles with varying shapes and sizes were observed.

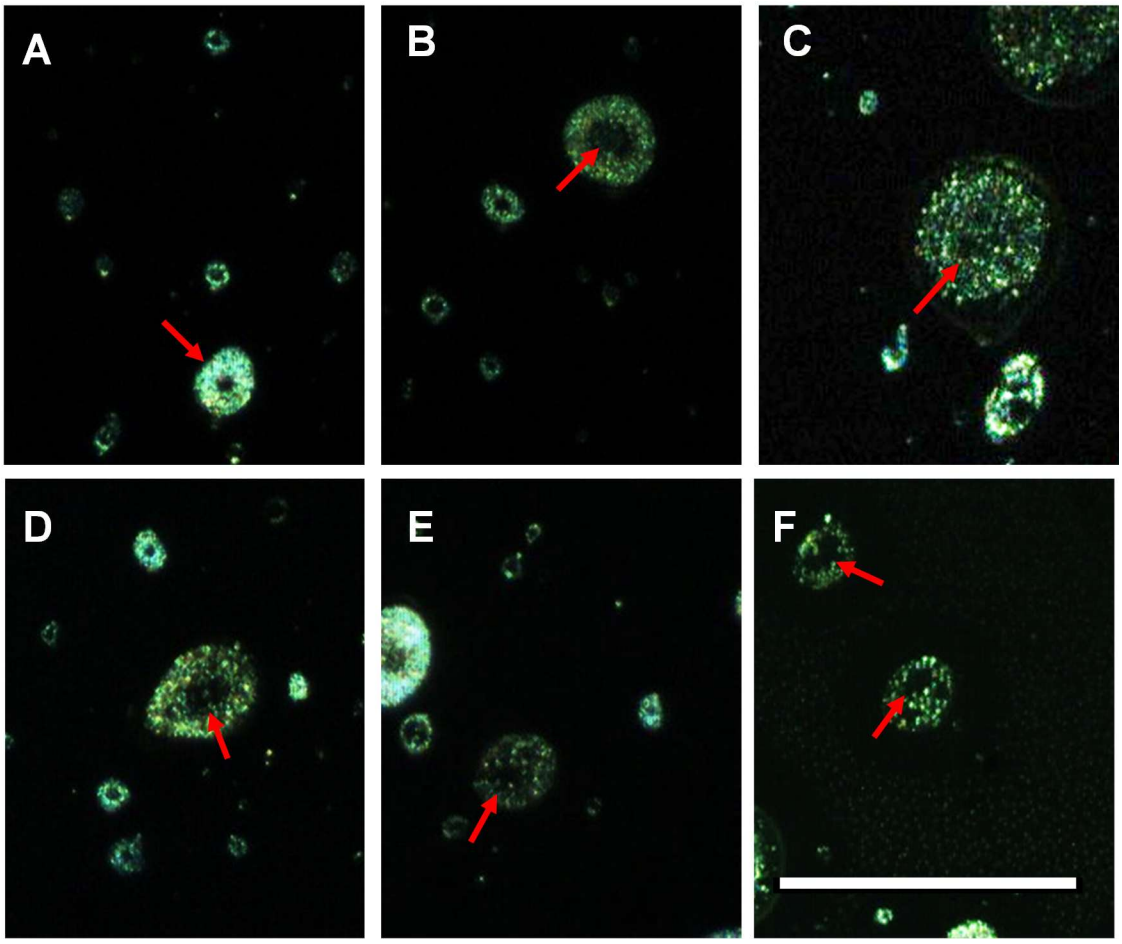

Fig. S12 Microvacuoles observed in protein-filled microdroplets. Droplets having vacuoles are indicated by red arrows. Fluorescein isothiocyanate (FITC)-labeled bovine serum albumin (BSA) was used as an analyte. Several droplets were found to have distorted shapes as observed previously in case of nanoparticles containing droplets. The scale bar is 250 μm.

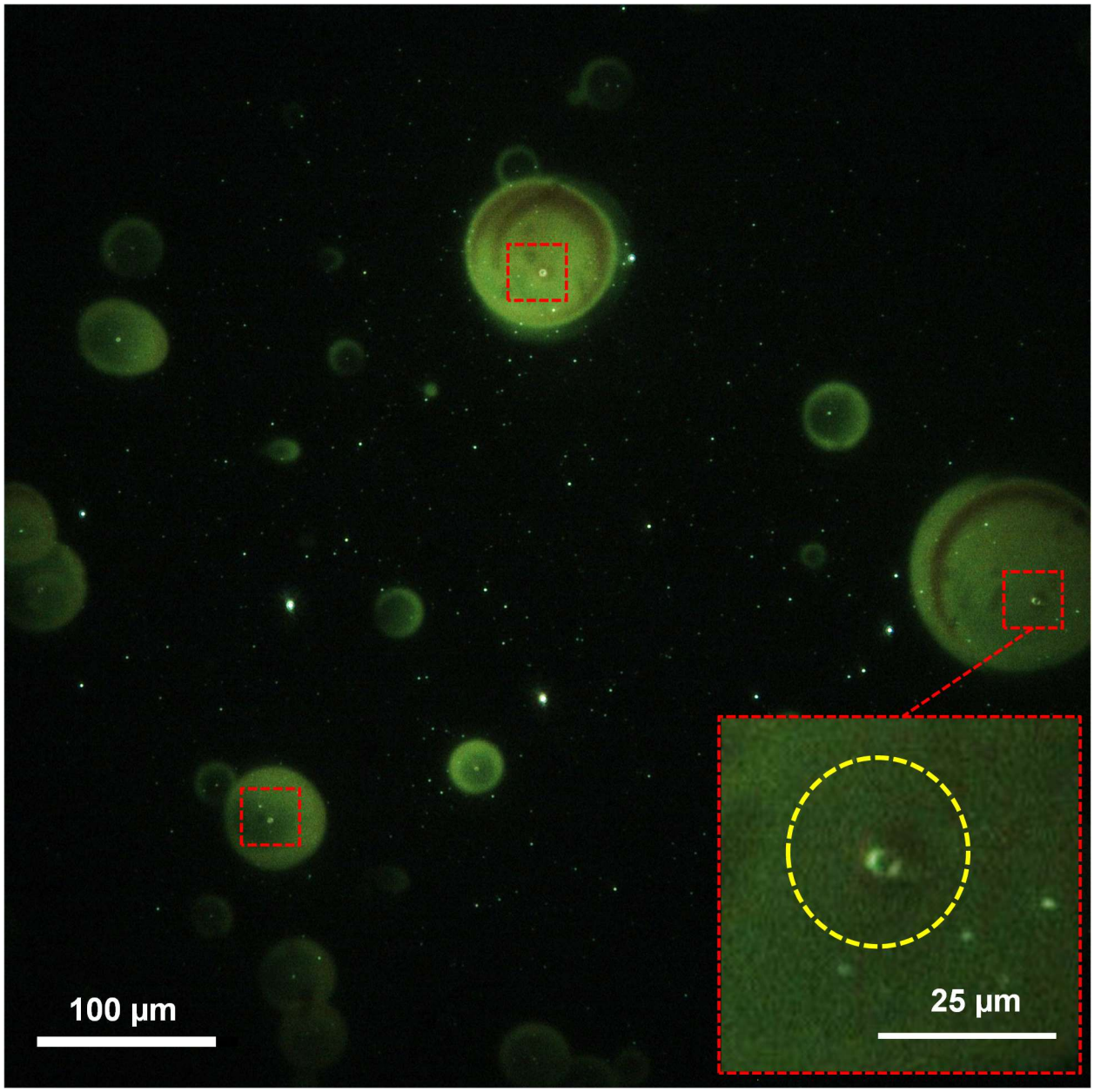

Fig. S13 Fluorescence image of microdroplets containing R6G after degassing of the solution. The degassing was performed by freezing the solution at -80 ºC followed by melting it at room temperature under vacuum. The image contains several droplets but only very few are found to have bubbles that are marked with red squares. The scale bar is 100 µm.